PERFORMANCE CHARACTERISTICS OF HCFC-123 EJECTOR REFRIGERATION CYCLES

DA-WEN SUN

Department of Agricultural and Food Engineering, University College Dublin, The National University of Ireland, Earlsfort Terrace Dublin 2, Ireland

AND

IAN W. EAMES

Institute of Building Technology, The University of Nottingham, Nottingham NG7 2RD, U.K.

SUMMARY

Ejector refrigeration systems can use low grade thermal energy, at temperatures as low as 60 °C, to provide space cooling. Since this waste energy is widely available and the cost of its supply is negligible in many cases, cooling costs can be lower than conventional systems, which makes the method very attractive. The present study describes a computer simulation model for ejector refrigeration systems that was developed using an existing ejector theory. This model allows for internal irreversibilities within the ejector to be included and caters for the addition of a regenerator and a precooler for improving the system coefficient of performance. The study shows that HCFC-123 is a suitable replacement for CFC-11 in this application. Results also indicate that the use of a variable geometry ejector can maintain the optimum performance of refrigeration systems when operating conditions change.

KEY WORDS: heat pumps; ejector; refrigeration; HCFC-123; computer simulation; CFC-11; variable geometry ejector

1. INTRODUCTION

Air conditioning and refrigeration play important roles in modern life, having applications in providing human comfort, in food processing and storage and in many industrial processes. These applications are dominated by mechanical vapour compression cycles because of their relatively low capital cost. However, these systems are generally powered by mains electricity supplied by power stations burning fossil fuels. The large amount of primary energy consumed by these systems is significant. On the other hand, thermal energy powered systems that can utilize waste heat or solar, biomass or geothermal energy can be useful alternatives. Inexpensive thermal energy sources can make heat powered refrigeration a viable and economic proposition.

There already exist two main heat powered systems that can operate using low grade heat: absorption cycles and desiccant cycles. LiBr–water and aqua–ammonia absorption machines are commercially available, but their construction and maintenance requires specialized skills. While desiccant systems are used in arid areas only and hence their capital cost is high.

This paper discusses a third alternative, i.e. the ejector refrigeration cycle. An ejector refrigeration cycle can utilize thermal energy at temperature levels upwards from 60 °C. A large portion of industrial waste heat (up to 60% of the primary energy input) is rejected at temperatures between 60 °C and 90 °C. Also, heat energy at these temperatures is available from such sources as flat plate solar collectors and exhausts from automobiles. The promotion of the utilization of waste thermal energy is a target area for our research into ejector refrigeration systems and an aim of this paper.

The first ejector system for cooling and refrigeration, which dates back to the early 1900s used water as refrigerant (ASHRAE, 1979). Because of the very few moving parts involved, such a system is very

reliable. A drawback of steam ejector systems is the high temperature source needed to power them and the large dimensions of the ejectors used. This confined their application to air-conditioning large buildings. Therefore, after their first wave of popularity in the 1930s, steam jet refrigeration units were supplanted by more compact electricity powered vapour compression machines. Many attempts have been made to make ejector refrigeration systems viable again by using more suitable halocarbon compound refrigerants (Sun and Eames, 1995). The earliest research on these systems was carried out by Mizrahi et al. (1957), who pointed out that thermal energy at 60 °C could be used to generate cooling. However, higher temperatures up to 90 °C are thought to be more appropriate for air conditioning (Sun and Eames, 1995). Since the work of Mizrahi et al., much research has been carried out on utilizing industrial low grade waste heat (Tyagi and Murty, 1985; Chen and Hsu, 1987), waste heat from automobile engine exhausts (Chen, 1978; Hamner, 1978, 1980) and solar energy (Zeren et al. 1979; Zeren, 1982; Zeren and Holmes, 1982; Shchetinina et al., 1987a,b). The most recent detailed research was carried out by Sokolov and Hershgal (1990a,b, 1991, 1993a,b) in which they used a double ejector system enhanced by a pressure booster to improve the part-load performance of their experimental system and to smooth the fluctuations in working conditions. They also considered using solar energy instead of waste thermal energy to power the system.

The most important research on ejector refrigeration systems, using halocarbon compounds, is summarized in Table 1. From the research papers listed in Table 1, the halocarbon refrigerant CFC-11 is clearly superior from the following thermodynamic standpoints. First, CFC-11 has a boiling point at atmospheric pressure of 23·7 °C — hence the condenser pressure may be just 0·5 bar above atmospheric pressure. This makes low pressure ejector refrigeration systems easy to design and maintain. Secondly, CFC-11 has a large vapour specific volume; hence the size of ejectors is larger for small experimental units than those using other refrigerants such as CFC-12. This makes ejectors easy to design and manufacture, especially in respect of the primary nozzles. However, CFC-11 has the largest ozone depletion potential (ODP), i.e. 1·0 of all CFCs. Therefore, the production and import of CFC-11 ceased at the end of 1994 and the need for a replacement is inevitable. It is well recognized that HCFC-123 is the most likely short-to-medium-term replacement for CFC-11. The reasons for this are that HCFC-123 has a similar boiling point (i.e. 27·8 °C) at atmospheric pressure and therefore, condenser pressures may be just 0·5 bar above atmospheric pressure as well. Also, HCFC-123 has a similarly large vapour specific volume. Furthermore, the ODP for HCFC-123 is 0·02 and hence it is a recognized environmentally-friendly refrigerant. HCFC-123 is the only alternative fluid presently on the market that could operate in a similar

Table 1. Summary of the research into ejector refrigeration systems using halocarbon compounds

Reference	Fluid	Method†	Temperature Range (°C)
Mizrahi et al. (1957)	R12, R22	T	$T_e = -15, T_c = 30, T_g = 60$
Chen (1978)	R113	T	$T_e = 7, T_c = 50, T_g = 76$
Hamner (1978, 1980)	R11	E, T	$T_e = 1·7-12·8, T_c = 29·4, T_g = 93·3$
Zeren et al. (1979), Zeren (1982), Zeren and Holmes (1982)	R12	E, T, S	$T_e = -9-17, T_c = 1·4-46, T_g = 54-82$
Faithfull (1984)	R11	E	$T_e = -5-15, T_c = 32, T_g = 87$
Tyagi and Murty (1985)	R11, R113	T	$T_e = 0-5, T_c = 30-35, T_g = 70-90$
Huang et al. (1985)	R113	E, T	$T_e = 5·2-14·9, T_c = 32-48, T_g = 65-80$
Shchetinina et al. (1987a,b)	R142	E, S	$T_e = 8-15, T_c = 40, T_g = 73-80$
Chen and Hsu (1987)	R11	T	$T_e = -1-21, T_c = 32-54, T_g = 82-104$
Sokolov and Hershgal (1990a,b, 1991)	R114	E, T	$T_e = 8·8, T_c = 43·3, T_g = 98·3$
Sokolov and Hershgal (1993a,b)	R114	T, S	$T_e = 4, T_c = 30-40, T_g = 90-105$
Nahdi et al. (1993)	R11	E	$T_e = 5-15, T_c = 20-40, T_g = 90-110$
Lu et al. (1993)	R11	T	$T_e = -6-12, T_c = 18-37, T_g = 82-148$

†T = theoretical; E = experimental; S = solar powered.

way as CFC-11. Therefore, in the present study an evaluation of the suitability of HCFC-123 as a replacement for CFC-11 in the context of ejector refrigeration is undertaken.

The performance of an ejector refrigerant system depends mainly on the design of the ejector. The optimum geometry of an ejector is normally determined by the operating conditions of the system. A computer simulation of such a system can provide the optimum operating conditions and design data; therefore, this is an important and necessary study. For the present study, a computer simulation model for the ejector refrigeration cycle was developed and used to analyze the effects of the operating temperatures, the efficiencies of the ejector components and practical methods of coefficient of performance improvement.

2. ANALYSIS OF EJECTOR REFRIGERATION CYCLES

Referring to Figure 1, the ejector compression cycle consists of a power sub-cycle 1-2-3-4-5-6-1 and a refrigeration sub-cycle 8-9-10-3-4-5-7-8 as illustrated in the pressure–enthalpy diagram in Figure 1(b).
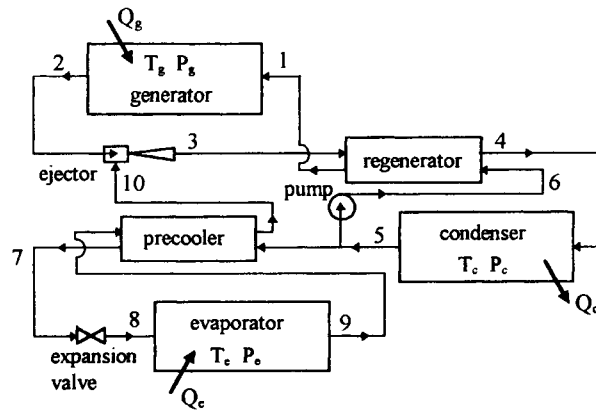
(a)
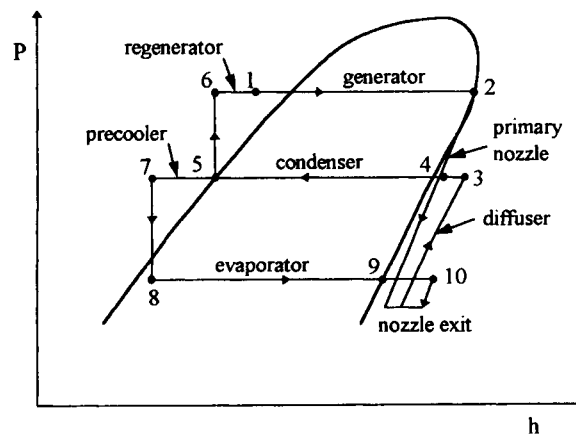
(b)

Figure 1. Schematic diagram of ejector refrigeration system
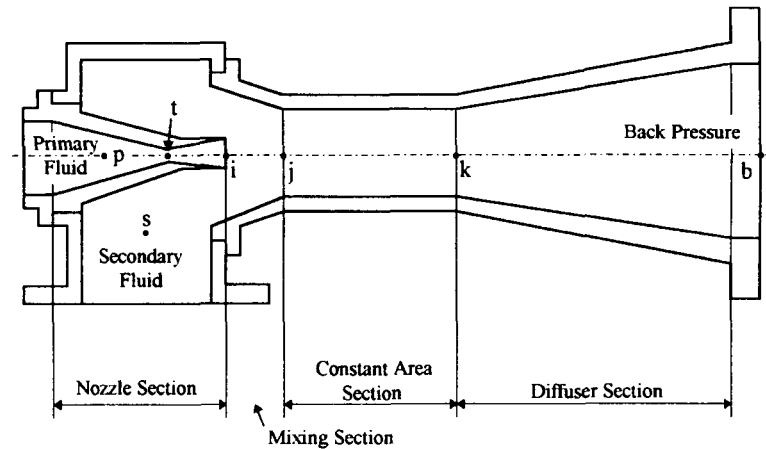
(a)
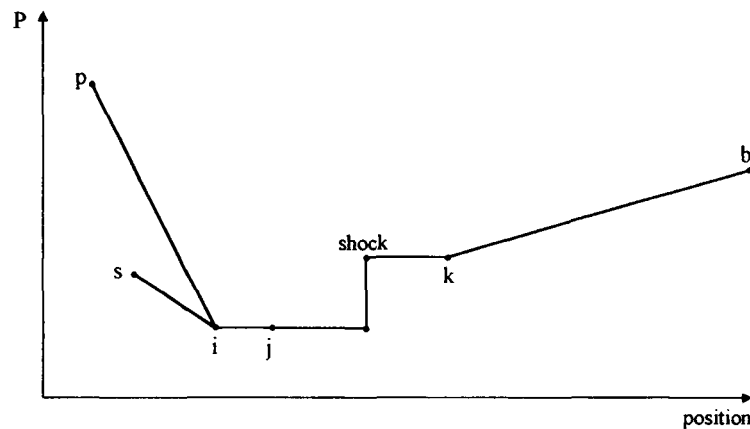
(b)

Figure 2. Ejector structure

The ejector in Figure 1 is shown in detail in Figure 2. In the power sub-cycle, low grade heat Q_g is delivered to the generator, where liquid refrigerant at state point '1' is vaporized at high pressure to state point '2'. This vapour (the primary, or driving, fluid) flows through the primary convergent–divergent ejector nozzle and enters the mixing section at point 'i' in Figure 2. The low pressure caused by this expansion induces the vapour (the secondary, or driven, fluid) from the evaporator at state point '10' in Figure 1. The primary and secondary fluids then combine at i-j-k and undergo a pressure recovery process j-k-b in the diffuser section. The combined stream at state '3' flows to the condenser and leaving at state '5', the heat of condensation Q_c is rejected to the environment. Finally, the condensate is pumped back to the generator '6' to complete the Rankine cycle. In the refrigeration sub-cycle, the condensate '5' from the condenser is expanded through a throttling valve to a low pressure state '8' and enters the evaporator from where it is evaporated to produce the necessary cooling effect Q_e. Refrigerant vapour at '10' is then entrained and mixed with the primary fluid and the combined stream is compressed '3' and condensed to state '5', thus completing the refrigeration sub-cycle. Therefore, the power to drive the cycle is provided by absorbing heat from a high temperature resevoir (low grade heat source) at the generator and rejecting heat at a lower temperature environment sink, thus producing the necessary power to drive the

refrigeration sub-cycle. The state points 6-1/3-4 and 5-7/9-10 in Figure 1 represent the regenerator and precooler, respectively. The addition of these components will be shown to increase system efficiency.

The thermodynamic performance of the ejector compression cycle is measured by a coefficient of performance (COP), defined as the ratio between the useful cooling or refrigeration effect at the evaporator to the gross energy input into the cycle required to produce the cooling effect. Therefore COP is given by

$$COP = Q_e/(Q_g + W_{me})$$ (1)

The maximum COP can only be obtained if the cycle is completely reversible. Its value can be determined by considering a Carnot refrigerator that operates between the condenser and the evaporator temperatures, driven by a Carnot heat engine that operates between the generator and condenser temperatures. Therefore, the maximum COP for an ejector cycle refrigerator is given by

$$COP_{max} = \frac{T_g - T_c}{T_g} \frac{T_e}{T_c - T_e}$$ (2)

The maximum COP given by an ideal reversible cycle can be determined directly from equation (2). However, the actual COP can only be calculated from equation (1) when the entrainment ratio of the ejector is known.

The operation of an ejector refrigeration cycle is normally characterized by the generator, condenser and evaporator temperatures and the total refrigerant mass flow through the generator m_0. Beginning with the generator, the high pressure vapour at state '2', entering the ejector, is given by the following functional relationships:

$$T_2 = T(T_g), \quad P_2 = P(T_g), \quad h_2 = h(T_g)$$ (3)

The low pressure vapour at state (9) can be calculated from the evaporator temperature:

$$T_9 = T(T_e), \quad P_9 = P(T_e), \quad h_9 = h(T_e)$$ (4)

and the condensed liquid at state (5) emerging from the condenser is determined by

$$T_5 = T(T_c), \quad P_5 = P(T_c), \quad h_5 = h(T_c)$$ (5)

If the effectiveness of the precooler is E_{pc}, then the fluid in states '10' and '7' is derived by using the above values as follows:

$$T_{10} = E_{pc}T_5 + (1 - E_{pc})T_9, \quad P_{10} = P_9, \quad h_{10} = h(T_{10}, P_{10})$$ (6)

$$P_7 = P_5, \quad h_7 = h_5 + h_9 - h_{10}, \quad T_7 = T(P_7, h_7)$$ (7)

Given the properties in states '2', '10' and '3', the entrainment ratio of the ejector can be determined from the following explicit and functional relationships:

$$P_3 = P_5, \quad \omega = f(P_2, T_2, P_{10}, T_{10}, P_3, A_t/A_k), \quad h_3 = (h_2 + \omega h_{10})/(1 + \omega),$$
$$T_3 = T(P_3, h_3)$$ (8)

The determination of ω is described in the next section. The condensate is partly pumped to the regenerator; as a result, the enthalpy at '6' is increased:

$$P_6 = P_2, \quad h_6 = h_5 + (P_6 - P_5)v_5, \quad T_6 = T(P_6, h_6)$$ (9)

If the effectiveness of the regenerator is E_{rg}, then the fluid in states (4) and (1) can be derived as

$$T_4 = T_3 - E_{rg}(T_3 - T_6), \quad P_4 = P_3, \quad h_4 = h(T_4, P_4)$$ (10)

$$P_1 = P_2, \quad h_1 = h_6 + (1 + \omega)(h_4 - h_3), \quad T_1 = T(P_1, h_1)$$ (11)

Through the expansion valve, the fluid pressure is reduced from the intermediate pressure to the low pressure, therefore

$$P_8 = P_9, \quad h_8 = h_7, \quad T_8 = T(P_8, h_8)$$ (12)

The mass flow continuity around the cycle yields the following:

$$m_6 = m_1 = m_2 = m_0, \quad m_{10} = m_9 = m_8 = m_7 = \omega m_0, \quad m_5 = m_4 = m_3 = (1 + \omega)m_0 \tag{13}$$

In order to determine the COP of the cycle, the energy balances at the generator and evaporator are required:

$$Q_g = m_0(h_2 - h_1), \quad Q_e = \omega m_0(h_9 - h_g), \quad W_{me} = (P_6 - P_5)v_5 \tag{15}$$

By solving equations (3) to (14), the COP of the system can be calculated using equation (1). The heat rejected by the condenser can be also found by taking the heat balance over the condenser as

$$Q_c = (1 + \omega)m_0(h_4 - h_5) \tag{15}$$

3. ANALYSIS OF EJECTOR DESIGNS

With a knowledge of the refrigerant's thermodynamic properties, equations (1)–(15) can be solved simultaneously to give the performance of the system. the entrainment ratio ω (m_s/m_p) in equation (8), which gives the performance of the ejector, can be found using existing ejector design theories. There are two established analytical techniques for predicting the performance of ejector designs: constant area and constant pressure mixing methods. It has been shown that the latter gives superior performance (Sun and Eames, 1995), consequently the constant pressure mixing theory due to Keenan *et al.* (1950) was used in the present study. Figure 2 shows the typical structure of a constant pressure mixing ejector and its simplified axial pressure profiles.

The analysis is based on the following assumptions (refer to Figure 2):

(i) primary and secondary fluids have the same molecular weight and ratio of specific heats;
(ii) primary and secondary streams are supplied at zero velocities (i.e. stagnation conditions) at states 'p' and 's';
(iii) at section 'i', the two streams begin to mix and the static pressure across this section is assumed to be uniform; mixing occurs at constant pressure between 'i' and 'j';
(iv) transverse shocks may occur at any plane between 'j' and 'k'; and
(v) at state 'b' the velocity is zero (i.e. stagnation conditions).

The primary vapour expands irreversibly through the nozzle. During this process, a portion of available energy is transformed into kinetic energy, hence at the nozzle outlet the steady flow energy equation yields

$$h_p = h_{pi} + V_{pi}^2/2 \tag{16}$$

Here $h_p - h_{pi}$ is the actual static enthalpy change, which is smaller than the isentropic change. A nozzle isentropic efficiency η_n can be defined as

$$\eta_n = \frac{h_p - h_{pi}}{h_p - h_{pi}^s} \tag{17}$$

where $h_p - h_{pi}^s$ is the enthalpy change undergone during an isentropic expansion.

It is more convenient to express equation (16) in terms of Mach number. Therefore, equation (16) can be rewritten as

$$M_{pi} = \left\{ \frac{2\eta_n}{\gamma - 1} \left[\left(\frac{P_{op}}{P_i} \right)^{(\gamma - 1)/\gamma} - 1 \right] \right\}^{1/2} \tag{18}$$

Similarly, the Mach number of the secondary flow at the exit of the nozzle plane is given by

$$M_{si} = \left\{ \frac{2}{\gamma - 1} \left[\left(\frac{P_{os}}{P_i} \right)^{(\gamma - 1)/\gamma} - 1 \right] \right\}^{1/2} \tag{19}$$

After section 'i', the two streams begin to mix. Since constant pressure mixing is assumed, the mixing process is governed by the following one dimensional continuity, momentum and energy equations:

$$m_p + m_s = m \tag{20a}$$

$$m_p V_{pi} + m_s V_{si} = m V_j \tag{20b}$$

$$m_p H_{pi} + m_s H_{si} = m H_j \tag{20c}$$

These equations can be combined to give a value for M_j^* in terms of M_{pi}^*, M_{si}^* and other known terms:

$$M_j^* = \frac{M_{pi}^* + \omega M_{si}^* \tau^{1/2}}{[(1 + \omega\tau)(1 + \omega)]^{1/2}} \tag{21}$$

where $\tau = T_{os}/T_{op}$. The relationship between M and M^* is given by

$$M = \left[\frac{2M^{*2}}{\gamma + 1 - M^{*2}(\gamma - 1)} \right]^{1/2} \tag{22}$$

Therefore, the Mach number M_j of the mixed stream can be calculated directly from M_j^* using equation (22).

If $M_j > 1$, the mixed stream is assumed to undergo a supersonic transverse shock that changes the flow from a supersonic to a subsonic condition and simultaneously producing a sudden static pressure rise. When the ejector operates properly, this shock will occur in the constant area section j-k. The relation between the Mach number upstream and downstream of the shock is given by

$$M_k = \left\{ \frac{\left(\frac{2}{\gamma - 1}\right) + M_j^2}{\left(\frac{2}{\gamma - 1}\right)\gamma M_j^2 - 1} \right\}^{1/2} \tag{23}$$

and the static pressure ratio across the shock P_k/P_j is obtained by combining the conservation of mass and momentum equation as

$$\frac{P_k}{P_j} = \frac{1 + \gamma M_j^2}{1 + \gamma M_k^2} \tag{24}$$

In the diffuser, the subsonic mixed flow is compressed further until its velocity decreases to zero assumed at the exit of the diffuser. If a diffuser efficiency η_d similar to nozzle efficiency η_n defined in equation (17) is assumed, then the pressure lift in the diffuser section can be derived as

$$\frac{P_{ob}}{P_k} = \left[1 + \frac{\eta_d(\gamma - 1)}{2} M_k^2 \right]^{\gamma/(\gamma - 1)} \tag{25}$$

Owing to constant pressure mixing $P_j = P_i$, the total pressure lift across the ejector, P_{ob}/P_{os}, can be found from

$$\frac{P_{ob}}{P_{os}} = \left(\frac{P_{ob}}{P_k} \right) \left(\frac{P_k}{P_j} \right) \left(\frac{P_i}{P_{os}} \right) \tag{26}$$

The above equations are directly connected to the ejector geometry, A_t/A_k by the following equation:

$$\frac{A_t}{A_k} = \frac{P_{ob}}{P_{op}} \left[\frac{1}{(1 + \omega)(1 + \omega\tau)} \right]^{1/2} \frac{\left(\frac{P_k}{P_{ob}}\right)^{1/\gamma} \left\{ 1 - \left(\frac{P_k}{P_{ob}}\right)^{(\gamma-1)/\gamma} \right\}^{1/2}}{\left(\frac{2}{\gamma + 1}\right)^{1/(\gamma-1)} \left\{ 1 - \left(\frac{2}{\gamma + 1}\right) \right\}^{1/2}} \tag{27}$$

From equations (18)–(27), the entrainment ratio ω can be found by iteration. Very often equations (18)–(27) are used to optimize the ejector geometry A_t/A_k, which gives the maximum total pressure lift P_{ob}/P_{os} and entrainment ration ω.

During the simulation, the following equation is used to relate the pressures of the ejector to that of the other part of the system. The pressure and temperature losses by the associated pipes can be easily incorporated by including suitable coefficients in the following relation if necessary:

$$P_2 = P_{op}, \quad T_2 = T_{op}, \quad P_{10} = P_{os}, \quad T_{10} = T_{os}, \quad P_3 = P_{ob}, \quad m_0 = m_p \qquad (28)$$

4. RESULTS AND DISCUSSION

A computer simulation program has been developed based on the analyses described previously. HCFC-123 was selected as the refrigerant. Its thermodynamic properties, taken from standard tables, were fitted to a set of polynomial equations. The following simulation results are based on the ejector refrigeration system, without a regenerator and precooler ($E_{rg} = 0$, $E_{pc} = 0$), operating at reference temperatures of $T_e = 5\,°C$, $T_c = 30\,°C$ and $T_g = 80\,°C$ and with the ejector having efficiency values of $\eta_n = 0\cdot85$ and $\eta_d = 0\cdot85$. In the following discussion, when one parameter varies, the other parameters remain unchanged.

4.1 Effect of operating temperatures

In practice, operating temperatures will vary with the surrounding environmental conditions. For example, the generator temperature will depend on the source heat, the condenser temperature relates closely to atmospheric conditions and changes in the cooling load may cause the evaporator temperature to alter.

Figure 3 shows the effect of changes in generator temperature. Results suggest that an increase in T_g will be accompanied by a rise in COP caused by an increase in entrainment ratio. However, it is important to recognize that the ejector geometry (A_k/A_t) also needs to increase with T_g to provide sufficient flow area for the flow to expand, mix and compress as shown in Figure 3.
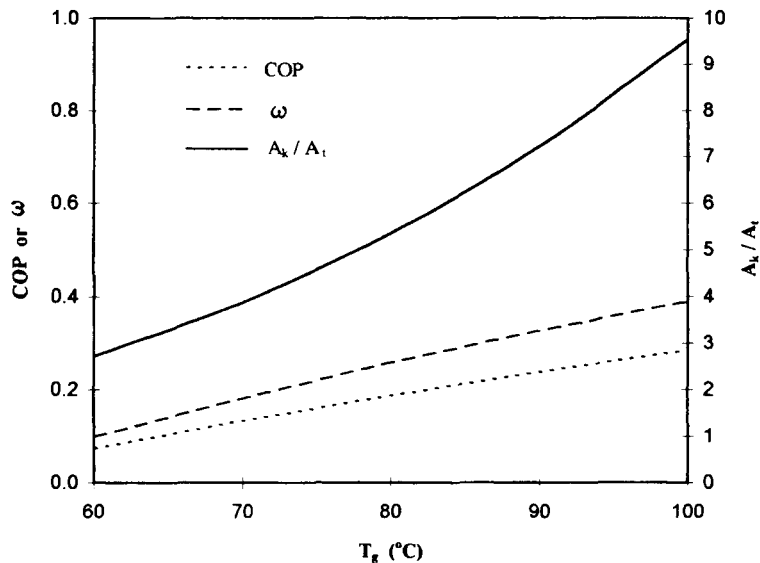
Figure 3. The effect of generator temperature

Experiments (Huang *et al.* 1985) have shown that ω decreases as T_g increases. Therefore, it seems that the variation of COP and ω in Figure 3 is in contradiction with the experimental results. However, in the experiments of Huang *et al.*, the geometry of the ejector was fixed with the result that as T_g (and hence P_g) rose, the flow through the primary nozzle became progressively more under-expanded. This means that the expansion of the primary fluid continues outside the nozzle outlet and, therefore, part of the mixing section (Figure 2) serves as the primary nozzle. As a result the flow area for the secondary fluid will reduce and this causes the entrainment ratio ω to fall. Under such operating conditions, the performance of the refrigeration system becomes increasingly more inefficient with increasing generator temperature.

In order to keep pace with changes in T_g, the geometry of the ejector ideally needs to be variable, as indicated in Figure 3. The flow rate through the primary nozzle is a function of the stagnation properties, flow area and Mach number as expressed by

$$m_0 = \frac{A_t M_{pi} P_{op}\left[\gamma/(RT_{op})\right]^{1/2}}{\left[1 + (\gamma - 1)M_{pt}^2/2\right]^{(\gamma + 1)/[2(\gamma - 1)]}} \tag{29}$$

Equation (29) indicates that for a given primary flow m_0 and perfect expansion (M_{pi} remains the design value), the nozzle throat area A_t needs to be decreased with rising P_{op}. At the same time, A_k also needs to be increased; as a result, the area ratio increases as shown in Figure 3.

Figure 4 shows the influence of the condenser temperature. An increase in T_c causes a decrease in ω and hence COP. This figure also illustrates the need for a variable geometry ejector to cope with changes in condenser temperature.

Munday and Bagster (1976, 1977) and Huang *et al.* (1985) have described the constant capacity characteristic of ejector refrigerator systems. This phenomenon results in COP and ω being independent of P_c when P_c is less than a certain critical value, and also the sharp fall in COP and ω (both to zero) when P_c is greater than this critical value. This constant capacity is caused by the choking of secondary fluid. The reason for this lies in the mixing process. As the primary and secondary streams enter the mixing section, they remain separated for some distance. The primary stream expands from the nozzle and fans out, effectively creating a convergent duct for the secondary fluid to accelerate within. This convergent duct is defined as an 'aerodynamically convergent nozzle' for the secondary fluid. When the
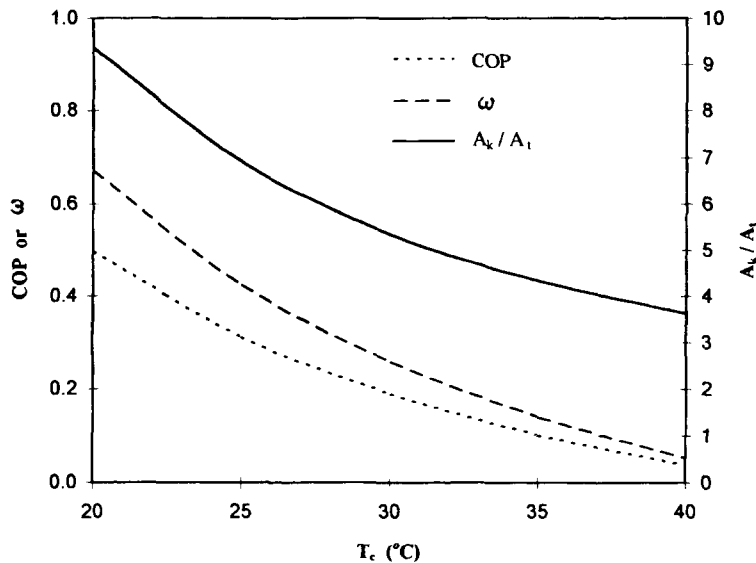
Figure 4. The effect of condenser temperature

secondary flow back pressure P_{sb} is reduced below a critical pressure P_{scr}, which is the pressure required to cause the fluid velocity to rise to the velocity of sound at the exit plane of the 'aerodynamically convergent nozzle', the secondary flow rate reaches a maximum and the flow chokes. Because the velocity of the secondary flow is sonic at the exit of the 'aerodynamic nozzle', a back pressure lower than the critical pressure cannot be sensed upstream, within the 'aerodynamic nozzle', and does not therefore affect the flow rate. On the other hand, when P_{sb} is increased higher than P_{scr}, the secondary flow will decrease. Further increase of P_{sb} to equal to P_{os} will cause the secondary flow to fall to zero, then the pressure distribution will be uniform along the 'aerodynamically convergent nozzle'.

Clearly, if the refrigeration system operates beyond the critical conditions, the efficiency (COP) of the system will be lower than it otherwise need be. As a result, some input energy at the generator will be wasted. Therefore, the geometry of the ejector should vary to avoid this situation. Since the geometry of the primary nozzle is determined by the thermodynamic state of the primary fluid at the generator, the area ratio variation shown in Figure 4 is actually the variation of the mixing throat A_k.

The effect of evaporator temperature is illustrated in Figure 5. It should be noted that with a rise in T_e, COP and ω also increase. However, T_e has much less influence on ejector geometry than either T_g or T_c. The reason for this is that the 'aerodynamically convergent nozzle' for the secondary fluid is generated by the supersonic primary stream and its aerodynamically choked area is only slightly influenced by P_g and P_e as illustrated by Huang et al. (1985). The reason for the increased of ω with P_e is that P_e causes an increase in secondary flow. To cope with this increase, the area of the mixing throat A_k needs to increase slightly.

From Figures 3 to 5, it is important to understand that to maintain optimum performance the geometry of the ejector needs to be varied, because it is difficult to control operating temperatures at their design values. This variation in geometry should first take place at the primary nozzle throat A_t and mixing chamber throat A_k.

4.2 Effect of ejector nozzle and diffuser irreversibilities

In most published research work, nozzle and diffuser flows are assumed to be isentropic (Keenan et al. 1950). However, this is not the case in practice. To examine the effect of non-isentropic flow on the performance of the refrigeration cycle, a parametric study was carried out to investigate the effect of changes in nozzle and diffuser isentropic efficiency.
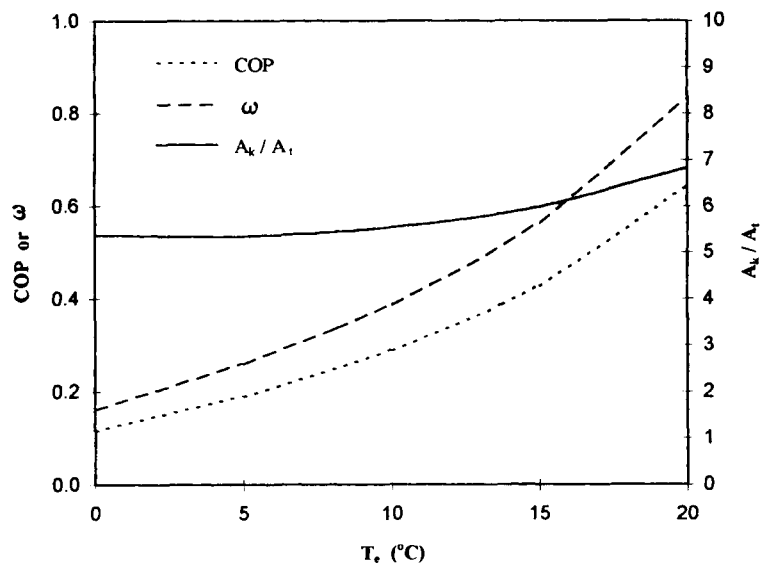
Figure 5. The effect of evaporator temperature

Figure 6 shows the effect of nozzle efficiency. It should be noted that nozzle efficiency has quite a severe influence on system COP. As shown in Figure 6, a fall in nozzle efficiency from 100% to 80% was predicted to result in a 16% decrease in COP. The reasons for this are the irreversible flow process in the nozzle resulting from the frictional effects which are mostly confined to the boundary layer, and by the effects of flow separation which induce strong turbulence near the nozzle wall. Flow separation occurs when the flow area increases faster than the fluid can expand. It is quite common for convergent–divergent nozzles to have efficiencies of less than 90% because of the irreversibilities in the divergent section. These can be reduced by carefully streamlining the nozzle contour and careful design of the divergent part of the nozzle. By this means, an efficiency of 90% or higher may be achieved. From a practical point of view, large nozzles are less difficult to manufacture and a better surface finish can be achieved than with small ones. Also, the boundary layer occupies a small portion of the total flow as nozzle size increases. The choice of the nozzle efficiency also affects the optimum design of the ejector, as shown in Figure 6. This effect is much less severe than that resulting from changes in operating conditions. However, care is needed when selecting efficiency data, particularly for small nozzles.

Diffuser efficiency also has effect on system performance, as illustrated in Figure 7. However, its influence is less significant compared with that of the nozzle. The causes of irreversibilities in the diffuser are similar to those in the primary nozzle. However, the irreversibility of the diffuser is more likely caused by flow separation.

4.3 Effect of COP improvement methods

It has been suggested that to increase refrigerator COP, a regenerator and a precooler might be added, as shown in Figure 1 (Huang et al., 1985; Chen and Hsu, 1987). The regenerator is used to preheat liquid refrigerant returning to the generator using the hot refrigerant from the ejector exhaust. The effect is to reduce the heat input to the generator. The precooler is used to cool the refrigerant liquid before it enters the evaporator via the expansion valve using the cold refrigerant vapour leaving the evaporator.

The effect of the regenerator effectiveness is illustrated in Figure 8. It is shown that, by adding a regenerator to the cycle, a 20% increase of COP may be theoretically possible. This approach suggests that significant improvement in cycle COP is possible. Technically, it is quite feasible for the regenerator to have an effectiveness as high as 90%; however, this needs to be justified economically.
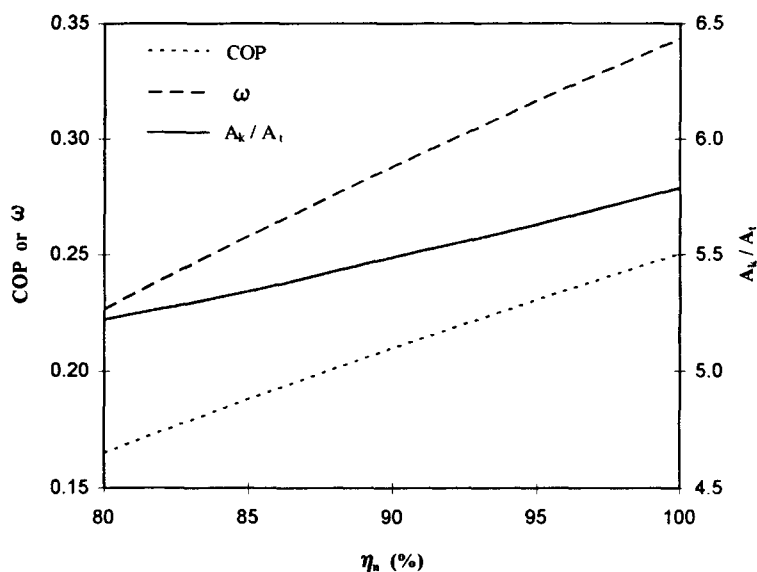
Figure 6. The effect of nozzle efficiency
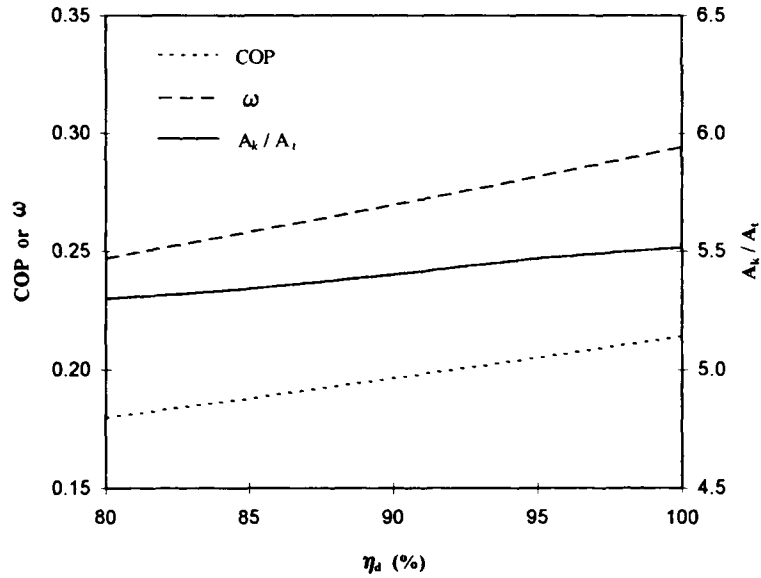
Figure 7. The effect of diffuser efficiency

The addition of a precooler to the cycle also improves system COP, as shown in Figure 9. However, the predicted improvement is significantly less than that achieved with the regenerator. If the capital cost of a precooler is considered, this small improvement in performance may not be sufficient to justify its inclusion in the cycle. From Figure 9, it is noted that adding a precooler actually reduces the entrainment ratio ω. This may be the reason for the lower efficiency upon adding the precooler. Actually, the secondary fluid is superheated (P_{0S} remains unchanged) when a precooler is used. This causes a reduction in the secondary flow in the 'aerodynamically convergent nozzle'. This phenomenon can be confirmed by careful study of equation (29).
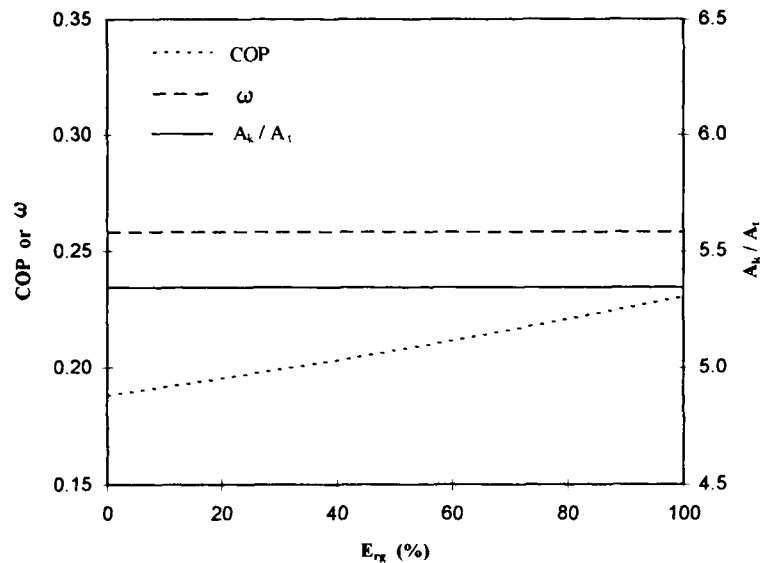
Figure 8. The effect of regenerator effectiveness
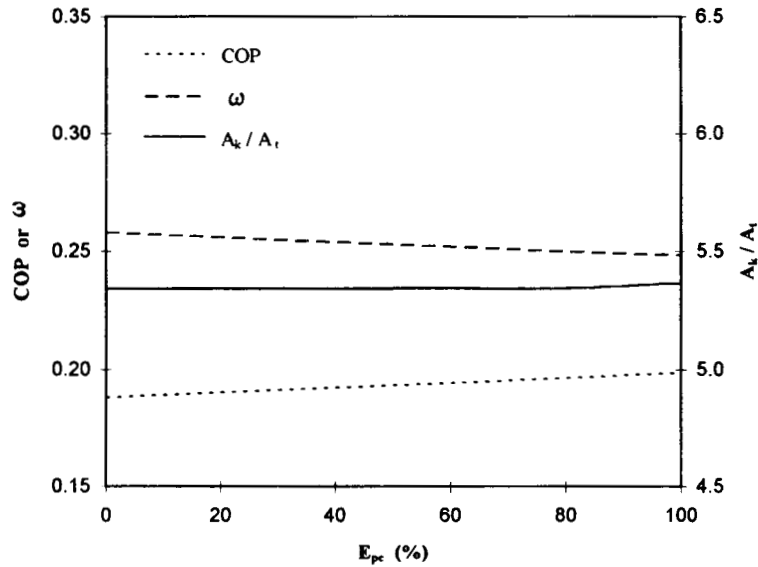
Figure 9. The effect of precooler effectiveness

5. CONCLUSIONS

An ejector refrigeration cycle operating on HCFC-123 can achieve a COP in the range 0·19 to 0·29 when operating at $T_e = 5-10\,°C$, $T_c = 30\,°C$ and $T_g = 80-90\,°C$. This COP can be improved by about 20% if a regenerator is introduced into the cycle. These prediced COP values are similar to those achieved by systems using CFC-11, reported by many researchers. Therefore, from a thermodynamic standpoint, HCFC-123 is a suitable replacement for CFC-11 in ejector refrigeration systems.

Generator and condenser operating temperatures have severe effects on the optimum design of ejectors. Therefore, for optimum operation it is necessary to use a variable geomery ejector to cope with variations in operating condition.

It is often assumed in the design of ejectors that the flows through the nozzle and diffuser are isentropic. This assumption affects the design of the ejector. Nozzle efficiency has more influence on the system COP than diffuser efficiency. Measures should be taken to improve the efficiencies of ejector nozzles and diffusers.

The introduction of a regenerator can bring about a significant improvement in system COP; however, the addition of a precooler has much less effect. In fact, its addition may not be economically justifiable.

NOMENCLATURE

A	=	area of cross section
E	=	effectiveness of precooler or regenerator
H	=	stagnation enthalpy
h	=	static enthalpy
m	=	mass flow rate
M	=	Mach number (actual velocity of fluid divided by local velocity of sound at the same state)
M^*	=	actual velocity of fluid divided by velocity of sound obtained with isentropic expansion from local stagnation conditions
P	=	static pressure
P_0	=	stagnation pressure
Q	=	heat

R	= gas constant
T	= static temperature
T_0	= stagnation temperature
V	= mean stream velocity
W	= work

Greek symbols

γ	= C_p/C_v, ratio of specific heats
η	= efficiency of nozzle or diffuser
ν	= specific volume
ω	= flow entrainment ratio, secondary stream to primary stream
τ	= ratio of stagnation temperatures, secondary stream to primary stream

Subscripts

c	= condenser
cr	= critical
d	= diffuser
e	= evaporator
g	= generator
k	= cross section of exit of constant area section shown in Figure 2
me	= mechanical
n	= nozzle
p	= primary fluid
pc	= precooler
rg	= regenerator
s	= secondary fluid
t	= cross section of minimum area of primary nozzle shown in Figure 2

REFERENCES

ASHRAE (1979). 'Steam-jet refrigeration equipment' in Equipment Handbook, Ch. 13, pp 13.1–13.6, ASHRAE, Atlanta Georgia, USA.

Chen, F. C. and Hsu, C.-T. (1987). 'Performance of ejector heat pumps', *Energy Res.*, 11, 289–300.

Chen, L.-T. (1978). 'A heat driven mobile refrigeration cycle analysis', *Energy Conversion*, 18(1), 25–29.

Faithfull, D. C. (1984). 'A combined Rankine and vapour compression cycle heat pump for teaching purposes, in *Proc. Int. Conf. on Directly Fired Heat Pumps — For use in Domestic and Commercial Premises*, P. W. Fitt and R. T. Moses (Eds), University of Bristol, U.K., 19–21 September 1984, Paper No. 3.1, pp. (3.1)1–7.

Hamner, R. H. (1978). 'An investigation of an ejector–compression refrigeration cycle and its applications to heating, cooling and energy conservation, Ph.D. thesis, University of Alabama, Birmingham, U.S.A.

Hamner, R. H. (1980). 'An alternate source of cooling: the ejector–compression heat pump', *ASHRAE J.*, 22 (July), 62–66.

Huang, B. J., Juang, C. B. and Hu, F. L. (1985). 'Ejector performance characteristics and design analysis of jet refrigeration system', *J. Engng Gas Turbines and Power, Trans. ASME*, 107, 792–802.

Keenan, J. H., Neumann, E. P. and Lustwerk, F. (1950). 'An investigation of ejector design by analysis and experiment', *J. Applied Mechanics, Trans. ASME*, 72, 299–309.

Lu, K.-T., Kou, H.-S. and Lan, T.-H. (1993). 'Geometrically and thermally non-optimum ejector heat pump analysis', *Energy Convers. Mgmt*, 34(12), 1287–1297.

Mizrahi, J., Solomiansky, M., Zisner, T. and Resnick, W. (1957). 'Ejector refrigeration from low temperature energy sources', *Bull. Res. Countil of Israel*, 6C, 1–8.

Munday, J. T. and Bagster, D. F. (1976). 'The choking phenomena in ejectors with particular reference to steam jet refrigeration', *Thermofluids Conf. of the National Committee on Thermodynamics and Fluid Mechanics of the Institution of Engineers of Australia*, Hobart, Tasmania, December 1976, National Conference Publication, Australia, pp. 84–88.

Munday, J. T. and Bagster, D. F. (1977). 'A new ejector theory applied to steam jet refrigeration', *Indust. Engng. Chem., Process Res. Dev.*, 16(4), 442–449.

Nahdi, E., Chamnpoussin, J. C., Hostache, G. and Cheron, J. (1993). 'Optimal geometric parameters of a cooling ejector–compressor', *Int. J. Refrig.*, 16(1), 67–72.

Shchetinina, N. A., Zhadan, S. Z. and Petrenko, V. A. (1987a). 'Experimental investigation of a solar–ejector Freon refrigerating machine', *Geliotekhnika*, 23(3), 66–69.

Shchetinina, N. A., Zhadan, S. Z. and Petrenko, V. A. (1987b). 'Comparison of the efficiency of various ways of heating the generator of a solar-ejector Freon refrigerating machine', *Geliotekhnika*, **23**(4), 71–74.

Sokolov, M. and Hershgal, D. (1990a). 'Enhanced ejector refrigeration cycles powered by low grade heat — Part 1: Systems characterisation', *Int. J. Refrig.*, **13**, 351–356.

Sokolov, M. and Hershgal, D. (1990b). 'Enhanced ejector refrigeration cycles powered by low grade heat — Part 2: Design procedures', *Int. J. Refrig.*, **13**, 357–363.

Sokolov, M. and Hershgal, D. (1991). 'Enhanced ejector refrigeration cycles powered by low grade heat — Part 3: Experimental results', *Int. J. Refrig.*, **14**, 24–31.

Sokolov, M. and Hershgal, D. (1993a). 'Optimal coupling and feasibility of a solar-powered year-round ejector air conditioner', *Solar Energy*, **50**(6), 507–516.

Sokolov, M. and Hershgal, D. (1993b). 'Solar-powered compression-enhanced ejector air conditioner', *Solar Energy*, **51**(3), 183–194.

Sun, Da-Wen and Eames, I. W. (1995). 'Recent developments in the design theories and applications of ejectors — a review', *J. Inst. Energy*, **68**, (475), 65–79.

Tyagi, K. P. and Murty, K. N. (1985). 'Ejector-compression systems for cooling: utilizing low grade waste heat', *Heat Recovery Systems*, **5**(6), 545–550.

Zeren, F. (1982). 'Freon 12 vapour compression jet pump solar cooling system', Ph.D. thesis, Texas A & M University, Texas, U.S.A.

Zeren, F. and Holmes, R. E. (1982). 'Performance evaluation for a jet pump solar cooling system', ASME Paper No. 81-WA/SOL-30.

Zeren, F., Holmes, R. E. and Jenkins, P. E. (1979). 'Design of Freon jet pump for use in a solar cooling system', ASME Paper No. 78-WA/SOL-15.